[13] Love, T. J., "An Experimental Investigation of Infra-red Scattering by Clouds of Particles," Rept. ARL-64-109, June 1964, Aerospace Research Labs.

[14] Williams, J. R., "Thermal Radiation Transport in Particle-Seeded Gases," *ANS Transactions*, Vol. 12, Dec. 1969, pp. 811–812.

[15] Mie, G. A., "Beitrage zur Optik truber Medien, Speziell Kolloidaler Metallosungen," *Annalen Der Physik*, Vol. 25, No. 3, 1908, pp. 377–445.

[16] Krascella, N. L., "Theoretical Investigations of the Absorption and Scattering Characteristics of Small Particles," Rept. C-910092-1, Sept. 1964, United Aircraft Research Labs.

[17] Aden, A. L., "Electromagnetic Scattering from Spheres with Sizes Comparable to the Wavelength," *Journal of Applied Physics*, Vol. 22, No. 5, 1951, pp. 601–605.

[18] Williams, J. R., Shenoy, A. S., and Clement, J. D., "Theoretical Calculations of Radiant Heat Transfer Properties of Particle-Seeded Gases," CR-1505, Feb. 1970, NASA.

[19] Plass, G. N., "Mie Scattering and Absorption Cross Sections for Aluminum Oxide and Magnesium Oxide," *Applied Optics*, Vol. 3, No. 7, 1964, pp. 867–872.

[20] Chi, J. W. H. and Landahl, C. E., "Hydrogen Reactions with Graphite Materials at High Temperatures and Pressures," *Nuclear Applications*, Vol. 4, March 1968, pp. 159–169.

[21] Clarke, J. T. and Fox, B. R., "Reaction of Graphite Filaments with Hydrogen above 2000°K," *Journal of Chemical Physics*, Vol. 46, No. 3, Feb. 1967, pp. 827–836.

[22] Duff, R. E. and Bauer, S. H., "Equilibrium Composition of the C/H Systems at Elevated Temperatures," *Journal of Chemical Physics*, Vol. 36, No. 7, April 1962, pp. 1754–1767.

[23] Cory, J. S. and Bennett, A., "Thermal Absorption in Seeded Gases," Rept. DAC-60779, Feb. 1969, Donald W. Douglas Labs.

[24] Stockham, L. W. and Love, T. J., "Monte Carlo Solution of Radiative Heat Transfer from a Finite Cylindrical Cloud of Particles," AIAA Paper 68-64, New York, 1968.

APRIL 1971 J. SPACECRAFT VOL. 8, NO. 4

Two-Dimensional Analysis of Transonic Gas-Particle Flows in Axisymmetric Nozzles

JOSEPH F. REGAN,* H. DOYLE THOMPSON,† AND RICHARD F. HOGLUND‡
Purdue University, Lafayette, Ind.

A recently developed two-dimensional technique for the calculation of isentropic perfect gas flowfields in axisymmetric nozzles of sharp wall curvature is used to provide initial values for a two-phase transonic flowfield calculation. The governing equations for the two-phase flow are expressed as finite-difference replacement equations that are solved by a numerical relaxation technique. A particle-free region appears and grows along the nozzle walls; the gas expansion in this region is regarded as isentropic to the predetermined local value of static pressure. Calculated flowfields and particle trajectories are presented for two families of nozzle contours and three particle sizes, and compared with the frequently employed constant-fractional-lag-mixture (CFLM) assumption and with calculations[6] based on a combination of the Sauer approximation to transonic flows and the CFLM assumption. Appreciable differences are found, especially in near-wall regions. The propagation of these differences through the supersonic nozzle flow is demonstrated.

Nomenclature

C_d = particle drag coefficient
C_P = specific heat at constant pressure
D = diameter
F = variable particle drag factor
G = variable particle heat-transfer factor
m = density per unit volume of particle
M = Mach number
P = pressure
R = gas constant
Re = Reynolds number
Rs = ratio of nozzle wall radius of curvature to throat radius
T = temperature
u = x-direction gas velocity component
v = y-direction gas velocity component
W = speed
x = axial coordinate along nozzle axis
y = radial coordinate measured from nozzle axis
γ = isentropic exponent
θ = streamline angle with respect to nozzle axis
μ = viscosity coefficient
ρ = density per unit volume of gas-particle mixture
Φ = particle-to-gas mass flow ratio

Subscripts§

g = gas property
o = total condition
p = particle property

Presented as Paper 69-572 at the AIAA 5th Propulsion Joint Specialist Conference, U.S. Air Force Academy, Colo., June 9–13, 1969; submitted October 20, 1969; revision received August 26, 1970. The authors gratefully acknowledge the assistance of G. Johnson of Purdue University, who made the supersonic nozzle performance calculations using the TRW computer program, and T. F. Zupnik of Pratt and Whitney Aircraft, who provided the perfect gas transonic flow program and useful consultation in understanding its logic and operation. Appreciation is also extended to J. D. Hoffman of Purdue University for his stimulating discussions throughout the course of the investigation.

* Colonel, U.S. Air Force; presently Director, Ramjet Division, Aero Propulsion Laboratory, Wright-Patterson Air Force Base, Ohio.

† Associate Professor of Mechanical Engineering. Member AIAA.

‡ Associate Professor and Director of Project SQUID; presently Manager, Physics and Applied Mechanics Department, Atlantic Research Corporation, Alexandria, Va. Associate Fellow AIAA.

§ Sub-subscript x or y denotes differentiation.

Introduction

IT now has been established both theoretically[1] and experimentally[2] that neither one-dimensional calculation techniques nor attempts to introduce two-dimensionality, via

series expansion or perturbations, give valid results for the flowfield in the throat region of axisymmetric nozzles of relatively sharp wall curvature. Rocket nozzles generally employ throat radii of curvature sufficiently small that realistic transonic flowfield solutions cannot be generated by these techniques, which fail to account for the influence of the upstream nozzle contour.

Recently, several two-dimensional techniques have been developed for the analysis of the homentropic flow of perfect gases in the throat region of nozzles with sharp wall curvature. Two of these techniques[1,3] are extensions of the method of lines introduced by Freidrichs.[4] They are inverse techniques in the sense that they calculate a boundary (wall) contour for a given axial velocity distribution, and depend on iterations and experience-generated correlations for matching of the calculated boundary to the desired wall contour. Only one of these programs[3] is available to external users, having been developed under government contract. A third program,[5] which involves the solution of hyperbolic time-dependent equations, has not reached the point of development at which it is available in operational form to external users.

Existing analyses of the flow of two-phase mixtures in the throat regions of axisymmetric nozzles[6,7] rely heavily on one-dimensional concepts, specifically, the constant-lag-mixture assumption. The most widely used calculational program, developed by Kliegel and Nickerson at TRW,[6] assumes (consistently) the existence of both a linear velocity profile and constant fractional lag in the throat region to give the gas flowfield, which results in a parabolic sonic line. Just as in the perfect gas case, these assumptions are inapplicable to nozzles of sharp wall curvature; the accuracy of the constant-fractional-lag approximation in two dimensions never has been tested.

Current engineering problems, such as plume studies related to infrared and optical signatures, electron generation, exhaust impingement, and nozzle impingement and heat transfer have created an additional need for accurate, detailed analyses of nozzle and plume flowfields. Particle trajectories and temperatures are particularly important in several of these problems. In a two-phase flow these properties are both boundary and history dependent, and the local accuracy of the subsonic and transonic flowfield affects directly the accuracy of calculated properties in the downstream supersonic flowfield.

The objective of the present study is to establish a method for determining improved initial values for a two-phase supersonic flowfield calculation including the effects of both upstream history and flow boundaries. Using initial flowfield data generated for the transonic flow of isentropic perfect gases in axisymmetric nozzles, an iterative numerical technique is developed for the incorporation of two-phase flow effects. This calculation technique is then used to investigate the sensitivity of the local details of transonic gas-particle flow to the coupled two-dimensional effects of nozzle shape and particle size. Additional details and program listings are available in Ref. 8.

Governing Equations

The conservation equations governing the steady, axisymmetric flow of gas-particle mixtures are derived in Refs. 7 and 9. The assumptions involved in these derivations are the following. 1) The total mass and total energy of the system remain constant. 2) The gas is inviscid except for its iteractions with the condensed particles. 3) The volume occupied by the condensed particles is negligible. 4) The thermal (Brownian) motion of the condensed particles is negligible. 5) The condensed particles do not interact. 6) The drag and heat-transfer characteristics of an actual shape and size distribution of particles can be represented by spherical particles of a single size. 7) The internal temperature of each condensed particle is uniform. 8) Energy exchange between the gas and the condensed particles occurs only by convection. 9) The only forces on the condensed particles are viscous drag forces. 10) There is no mass transfer between the gas and the condensed phase during the nozzle expansion. 11) The gas phase is thermally and calorically perfect and the flow is chemically frozen. 12) The particles do not undergo a phase change in the region of the calculation.

Based on these assumptions, the following equations govern the gas-particle flow[6,7]:

gas-phase and particle-phase continuity equations

$$\rho_g u_{gx} + \rho_g u_{gy} + u_g \rho_{gx} + v_g \rho_{gy} + \rho_g v_g / y = 0 \quad (1)$$

$$\rho_p u_{px} + \rho_p u_{py} + u_p \rho_{px} + v_p \rho_{py} + \rho_p v_p / y = 0 \quad (2)$$

gas-phase axial and radial momentum equations

$$\rho_g [u_g u_{gx} + v_g u_{gy}] + P_{gx} + F\rho_p (u_g - u_p) = 0 \quad (3)$$

$$\rho_g [u_g v_{gx} + v_g v_{gy}] + P_{gy} + F\rho_p (v_g - v_p) = 0 \quad (4)$$

gas-phase energy equation

$$u_g P_{gx} + v_h P_{gy} - \gamma R T_g [u_g \rho_{gx} + v_g \rho_{gy}] - F\rho_p (\gamma - 1) \times [(u_g - u_p)^2 + (v_g - v_p)^2 + (G/F)(T_p - T_g)] = 0 \quad (5)$$

particle-phase axial and radial momentum equations

$$u_p u_{px} + v_p u_{py} = F(u_g - u_p), \; u_p v_{px} + v_p v_{py} = F(v_g - v_p) \quad (6)$$

particle-phase energy equation

$$u_p T_{px} + v_p T_{py} = -G(T_p - T_g)/c_{P_p} \quad (7)$$

gas-phase equation of state

$$P_g = \rho_g R T_g \quad (8)$$

The drag force and heat-transfer factors which appear in these equations are defined as

$$F \equiv 9\mu_g f_p / 2 m_p r_p^2 \quad (9)$$

$$G \equiv 3\mu_g g_p c_{P_g} / m_p Pr r_p^2 \quad (10)$$

where f_p and g_p are drag and heat-transfer factors, respectively, which may be allowed to vary as a function of local flowfield properties in accordance with an empirical relationship or tabulated data. The spherical particle drag coefficient table and empirical formulas used in the TRW program[6] also are used in the current investigation, so that results can readily be compared. These relationships are

$$f_p = C_d(1 + 2.52\bar{C})/(1 + 3.78\bar{C}) \quad (11)$$

$$g_p = C_d/(1 + 3.42 C_d \bar{C}/\gamma^{1/2} Pr) \quad (12)$$

where

$$\bar{C} \equiv \mu_g / \rho_g r_p (R T_g)^{1/2} \quad (13)$$

and

$$C_d = C_d(Re) \quad (14)$$

is found from tabulated data.

The local Reynolds number is based on the speed of the particle relative to the gas and is defined as

$$Re \equiv 2 r_p (W_g - W_p) \rho_g / \mu_g \quad (15)$$

where W_g and W_p are the gas and particle speeds.

The gas viscosity is a function of temperature

$$\mu_g = \mu_{go} [T_g / T_{go}]^{0.67} \quad (16)$$

and Euken's relationship is used to compute the Prandtl number, which remains constant for a perfect gas at about 0.8

$$Pr = 4\gamma / 9\gamma - 5 \quad (17)$$

Computational Approach

There is no demonstrated mathematical method of solving the foregoing set of mixed-type quasi-linear partial differential equations. Although the governing equations for two-

phase flow are classed as nonlinear, the terms are no worse than quasi-linear, and the equations are of first order. The governing equations therefore can be rewritten in finite difference form as a set of linear algebraic equations when finite difference analogs are used to approximate the first-order partial derivatives. These algebraic equations are then used to derive an equivalent set of algebraic replacement equations in which a dependent variable is isolated on the left and its value is determined numerically from the remainder of the formula on the right of the equation. To obtain a solution for the flowfield, an initial flowfield is assumed from which the right side of the replacement equation can be evaluated. Then the replacement equations are evaluated for the dependent variables at all grid points and boundary points. The newly computed dependent variables are then used to update the right side of the replacement equations in an iterative solution.

The basic computational technique is a modified Gauss-Siedel[10] method for which only a single dependent variable, or a pair of dependent variables, in the case of velocity components, is computed at each pass. The same technique is then applied to the next dependent variable using the last computed values of all other dependent variables.

The successful applications of such a relaxation method requires tailoring of the method to the problem. Generally, absolute convergence is not possible, and a decrease in the change in all variables between successive iterations is considered equivalent to obtaining convergence. As a direct consequence, the solution accuracy is sensitive to the accuracy of the initial flow estimate. In formulating the relaxation procedure, the governing equations for the parameters which change most drastically are solved first.

The Initial Flowfield

A modified version of the Pratt and Whitney Subsonic-Transonic Flow Analysis Computer program[3] is used to generate initial flowfield data based on an equilibrium gas-particle mixture (EGPM). The solution is converted to a dimensional coordinate system comprised of streamlines, which are equally spaced at the inlet, and constant axial increments. A dimensional coordinate system is required for the relaxation procedure since the local properties in the dissipative flowfield are rate dependent and consequently position dependent.

The EGPM flowfield is calculated by regarding the two-phase fluid as a heavy perfect gas with a modified isentropic exponent ($\bar{\gamma}$) and modified molecular weight ($\bar{m}$) based on the over-all particle to gas-mass ratio (Φ)

$$\bar{m} = m/1 + \Phi, \bar{\gamma} = \gamma(1 + \Phi_c)/1 + \gamma\Phi_c \qquad (18)$$

where

$$\Phi_c = \Phi C_{P_p}/C_{P_g} \qquad (19)$$

$\bar{M}_s$ is the EGPM Mach number where the gas-phase Mach number M_g is unity

$$\bar{M}_s = \gamma(\bar{\gamma} + 1)(1 + \Phi)/\bar{\gamma}(1 + \gamma) \qquad (20)$$

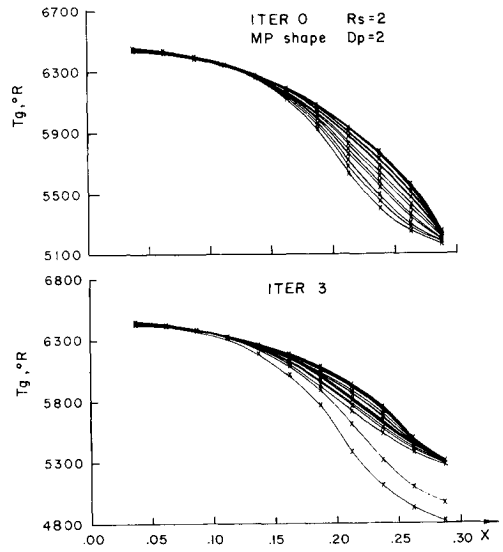

Fig. 2 Gas temperatures along streamlines.

The utility of this approach is that an approximate gas phase flowfield can be extracted by retaining the EGPM pressure, temperature, and velocity field values while using the gas phase molecular weight and isentropic exponent to determine M_g. The result is a gas flowfield in which the gas-phase sonic line is displaced downstream of the throat as occurs in a real dissipative flow.

Alternatively, a constant fractional-lag-mixture (CFLM) assumption[11] could be used to provide initial estimates of the flowfield. The equivalent isentropic exponent for a CFLM is always greater than that for an EGPM. The EGPM assumption is used in the present calculations to demonstrate convergence of the method for this case.

The Relaxation Procedure

In the relaxation procedure it is assumed that the static pressure field and the locations of the gas streamlines and gas phase grid point coordinates are constant at the EGPM values. It is also assumed that the gas velocity, density, and pressure gradients in the replacement equations do not vary from the EGPM values. The gas velocities, temperatures, and densities themselves, except those at the inlet boundary are allowed to vary to account for gas-particle interactions. The limiting particle streamline constitutes a boundary between the continuous two-phase flow region in which the flow is dissipative and the particle-free region in which the gas is assumed to be strictly adiabatic (i.e., the entropy is constant in each streamline but varies between streamlines).

To carry out the relaxation procedure, the governing differential Eqs. (3-7) are written as replacement equations and

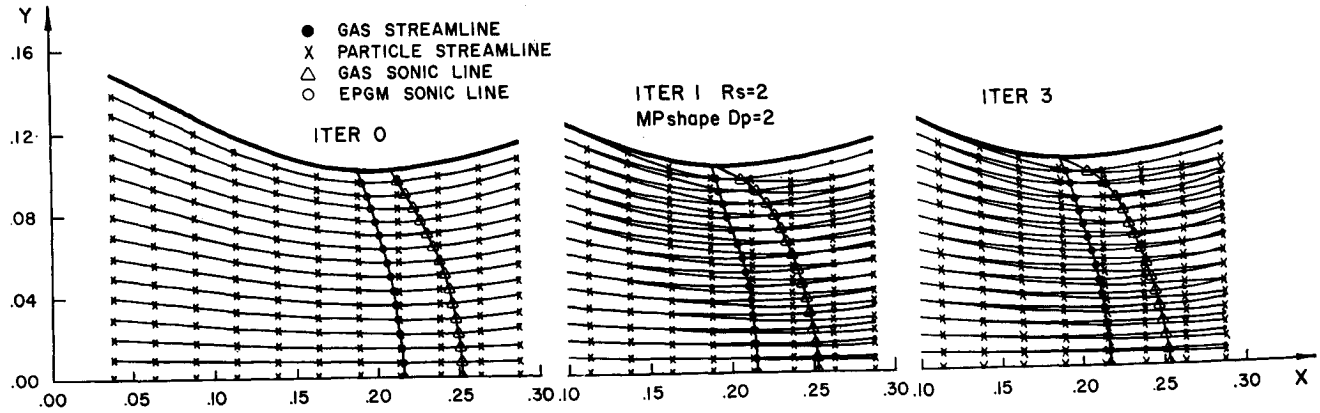

Fig. 1 Flowfield iterations; 2-μ particles.

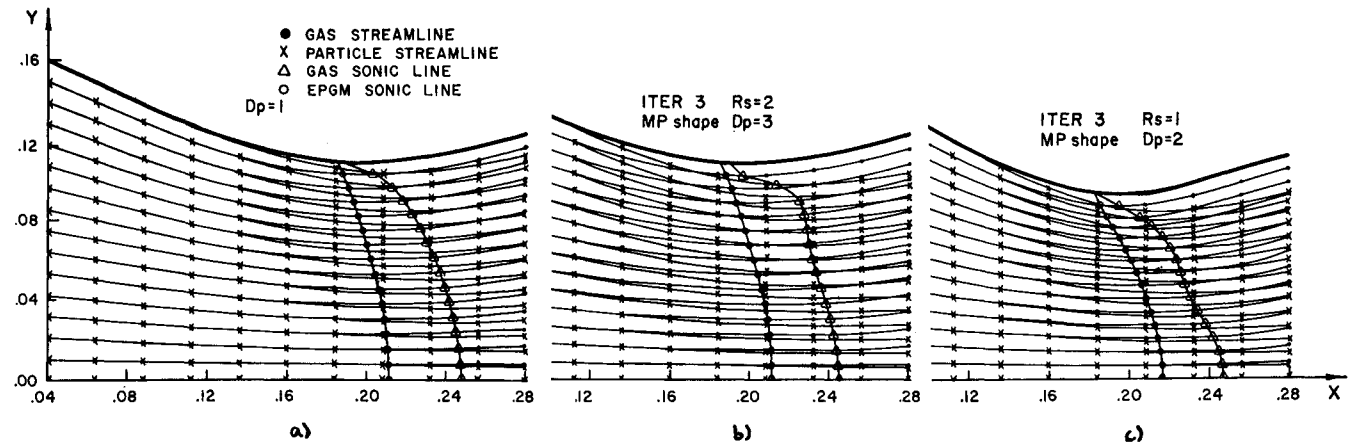

Fig. 3 Effects of different particle sizes and throat curvature ratios.

take the following form:

$$u_g = \frac{[F\rho_p u_p - P_{gx}][\rho_g v_{gy} + F\rho_p] - \rho_g u_{gy}[F\rho_p v_p - P_{gy}]}{[\rho_g v_{gy} + F\rho_p][\rho_g u_{gx} + F\rho_p] - \rho_g u_{gy}\rho_g v_{gx}} \tag{21}$$

$$v_g = \frac{[F\rho_p u_p - P_{gy}][\rho_g u_{gx} + F\rho_p] - \rho_g v_{gx}[F\rho_p u_p - P_{gx}]}{[\rho_g v_{gy} + F\rho_p][\rho_g u_{gx} + F\rho_p] - \rho_g u_{gy}\rho_g u_{gx}} \tag{22}$$

From Eq. (5),

$$T_g = \frac{(1-\gamma)\rho_p\{GT_p + F[(u_g - u_p)^2 + (v_g - v_p)^2] + u_g P_{gx} + u_g P_{gy}\}}{\gamma R[u_g\rho_{gx} + v_g\rho_{gy}] - G\rho_p(\gamma - 1)} \tag{23}$$

From Eq. (6),

$$u_p = \frac{F\{u_g[F + v_{py}] - v_g u_{py}\}}{\{[F + u_{px}][F + v_{py}]\} - u_{py}v_{px}} \tag{24}$$

$$v_p = \frac{F\{v_g[F + u_{px}] - u_g v_{px}\}}{\{[F + u_{px}][F + v_{py}]\} - u_{py}v_{px}} \tag{25}$$

The slope of a particle streamline can then be determined as

$$\tan\theta_p = \frac{v_p}{u_p} = \frac{v_g[F + u_{px}] - u_g v_{px}}{u_g[F + v_{py}] - v_g u_{py}} \tag{26}$$

And from Eq. (7)

$$T_p = T_g - G/c_{Pp}[u_p T_{px} + v_p T_{py}] \tag{27}$$

Following the general guide that the properties which differ most from the initial values should be calculated first, a relaxation procedure was developed consisting of the following iterative sequence of operations.

1) Calculate the particle velocity components u_p and v_p at the particle coordinate system grid points using Eqs. (24) and (25). The first-order derivatives are computed from initial flowfield values using numerical differentiation. The grid point "marching order" used throughout the computer program is to start at the known inlet boundary on the axis streamline and to march down one streamline to the exit before moving outward to the origin of the next streamline and repeating. Particle properties on the upstream boundary are allowed to vary.

2) Integrate the particle trajectories through the flowfield to determine new particle streamlines and coordinate system. Particle trajectories are integrated one at a time through the particle velocity field using the u_p, v_p, and $\tan\theta_p$ values calculated from Eqs. (24–26). The outermost particle streamline constitutes a boundary between the two-phase and particle-free regions.

3) Calculate particle density (ρ_p) at particle grid points. The particle density calculation satisfies the particle continuity Eq. (2).

4) Interpolate to find particle properties on gas coordinate system and gas properties on particle coordinate system.

5) Calculate particle temperature (T_p) at particle grid points using Eq. (27).

6) Recalculate particle trajectories and particle densities and reinterpolate. This step is an interation of steps 3, 4, and 5.

7) Calculate the gas velocity components u_g and v_g and the gas temperature T_g at the gas phase coordinate system grid points using Eqs. (21–23).

8) Calculate the gas velocity components, the gas temperature, and the gas density at the grid points in the particle-free region. The gas phase total pressure P_{go} and total temperature T_{go} are calculated for each gas streamline at the point of its intersection with the limiting particle streamline. These quantities remain constant along gas streamlines in the particle-free region. When taken together with an assumed invariance of the gas static pressure and streamline locations in the particle-free region, this permits the gas velocity components, temperature, and density to be computed from isentropic relationships.

9) Calculate the gas density ρ_g at gas phase coordinate system grid points in the two-phase regions. The gas density calculation satisfies the gas phase continuity Eq. (1).

10) Interpolate to find gas properties at all particle coordinate system grid points.

11) Determine the location of and local properties on a specified constant Mach number line or any specified initial value line.

12) Integrate particle and gas mass flows to independently verify that the gas and particle continuity Eqs. (1) and (2) have been satisfied. This step terminates one iteration of the relaxation process which becomes cyclic after the first iteration.

Results

The particle size distribution and the nozzle shape are two important parameters that affect the degree of two-dimensional nonequilibrium effects in gas-particle flows. The effects of other parameters, such as pressure level, total temperature, particle loading, and transport property values, have been studied previously. Therefore, the effects of nozzle shape and particle size were of primary concern in the present study.

Two families of nozzle shapes, the circular arc (CA) and a modified probability curve (MP), were investigated. All

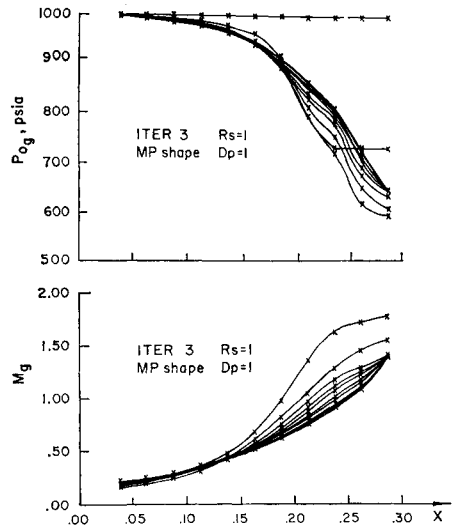

Fig. 4 Total pressures and gas Mach numbers along streamlines.

calculations were made for a nominal throat radius of 0.1 ft. For the circular arc contour, two values of wall curvature were investigated, 0.1 ft and 0.2 ft. These two values correspond to radius ratios (wall curvature radius/throat radius) of one and two. The radius ratio of one is significant since existing transonic solution techniques cannot handle this case. The solutions at a radius ratio of two provide results for comparison with other solution methods. Three grid size configurations were investigated to evaluate the sensitivity of the numerical methods to grid point spacing and distribution. Three typical particle sizes—1-, 2-, and 3-μ diam—were selected for investigation and comparison. This range of particle sizes includes the nominal size distributions expected in the transonic region of propulsion nozzles for contemporary solid propellant rockets. The reference combustion chamber equilibrium conditions were selected to duplicate those used in Ref. 6 so that output data could be compared most readily.

Successive iterations of the flowfield in the MP nozzle for a flow containing 2-μ diam particles (particle-to-gas mass flow rate of 0.4) are shown in Fig. 1. An 11-axial station, 16 streamline grid was employed. Comparison of the third iteration with the zeroth iteration (EGPM) shows that the EGPM assumption gives the sonic line location on the axis quite well, but provides a very poor estimate of sonic line location near the wall. This, of course, is because the particles depart from the gas streamlines (and the wall) in the region where the nozzle throat curvature becomes significant, leaving a particle-free region adjacent to the wall.

The effect of the adiabatic nature of the gas expansion in the particle-free region is illustrated in Fig. 2, where it is seen that gas temperatures along near-wall streamlines can differ by as much as 20% from the values calculated with the EGPM assumption. Since as much as 20% of the total mass flow passes through the particle-free region at the sonic line, these departures from the results of the EGPM (or CFLM) assumptions are significant.

Table 1 Fractional velocity and temperature lag ratios

	u_p/u_g		$T_o - T_p/T_o - T_g$	
	Streamline		Streamline	
Grid plane	1	11	1	11
1	0.95	0.93	0.91	0.86
2	0.93	0.92	0.87	0.86
3	0.92	0.91	0.86	0.84
4	0.92	0.90	0.85	0.83
5	0.91	0.89	0.81	0.81
6	0.91	0.89	0.81	0.81
7	0.90	0.88	0.81	0.78
8	0.90	0.88	0.81	0.78
9	0.90	0.89	0.80	0.79
10	0.89	0.88	0.77	0.80
11	0.87	0.89	0.74	0.82

The effects of different particle sizes are shown in Figs. 3a and 3b, which illustrate calculations for the same nozzle and mass flow rate considered above but with the particle size changed to 1-μ and 3-μ diam, respectively. Both the magnitude of nonequilibrium effects and the gradients (e.g., along the sonic line) increase as the particle size increases. Not surprisingly, the sonic line location is affected most strongly by two-dimensional effects in the 3-μ particle case. The "bulge" in the sonic line location near the outer part of the two-phase region (Fig. 3b) occurs because two-dimensional particle channeling is not uniform across the nozzle. The distances between particle streamlines near the limiting streamline are reduced more, relative to the distances between gas streamlines, than is the case for particle streamlines near the axis. The particle density thus is increased in the two-phase region near the limiting streamline, causing an increase in the local gas temperature (as much as 100°R at the sonic line; 200°R at the last grid point). The local increase in gas temperature raises the sonic speed. In addition, the increased drag of the particles on the gas in this region lowers the gas velocity. These two effects combine to shift the local sonic line location downstream.

Similar increases in both two-dimensional and nonequilibrium effects occur when the nozzle wall radius of curvature is decreased, as shown in Fig. 3c, for a 2-μ particle flow in a nozzle with a wall-to-thorat radius ratio of unity. A decrease in radius ratio from two to one substantially increases the size of the particle-free region and causes approximately a 25% increase in velocity lags at the sonic line along with a corresponding 68% increase in temperature lag (referenced to the no-lag values). Changes in the type of nozzle contour (MP to CA) caused much smaller effects (typically, $\frac{1}{2}$% changes in sonic line properties), substantiating the common assumption that the throat radius of curvature is the most important nozzle contour variable.

Typical plots of Mach number and total pressure profiles are shown in Fig. 4. Notice the growing total pressure "anti-

Table 2 Comparative initial value line data, $D_p = 2\mu$

	TRW program			Present calculation		
Location	Axis	LSL	Wall	Axis	LSL	Wall
x, ft	0.2592	0.2296	0.2250	0.2592	0.2299	0.2250
y, ft	0.0	0.0945	0.1016	0.0	0.0930	0.1016
P_g, psi	414	380	373	395	363	349
u_g, fps	4534	4702	4742	4694	5070	5776
v_g, fps	0.0	55.2	59.7	0.0	57.6	67.1
ρ_p, lbm/ft^3	0.0627	0.0636	...	0.0642	0.0668	...
u_p, fps	4074	4118	...	4112	4385	...
v_p, fps	0.0	14.7	...	0.0	21.0	...

Table 3 Comparative data at nozzle exit characteristics, $D_p = 2\mu$

Location	TRW transonic program			Present transonic program		
	Axis	LSL	Wall	Axis	LSL	Wall
x, ft	1.449	2.597	2.727	1.424	2.537	2.726
y, ft	0.0	0.5631	0.6326	0.0	0.5430	0.6325
M_g	2.576	3.853	4.270	2.573	3.936	4.476
T_g, °R	3286	2037	1791	3279	2008	1705
T_p, °R	3879	2433	...	3863	2375	...
W_p, fps	8656	10255	...	8624	10410	...
θ_p, deg	0.0	11.33	...	0.0	11.20	...
I_{sp}, sec	...	...	317.67	...	...	322.48

boundary layer" or region of reduced dissipation near the wall, corresponding to the growth of the particle-free region.

Typical fractional lags determined by the present calculation method are given in Table 1 for the MP nozzle, radius ratio 2, 2-μ particle case. Although the fractional lag values vary by as much as $\pm 10\%$ from the mean, the values on the axis at the nozzle minimum area section (streamline 1 at grid plane 7) are fairly representative of the mean.

Since the objective of this study was to provide improved values of downstream nozzle and plume flow properties, a comparison was made with results obtained from the Kliegel-Nickerson program.[6] Calculated properties were compared at a slightly supersonic initial value line (Table 2) and also at the exit of a 40:1 expansion ratio nozzle (Table 3). Supersonic flowfield computations for both cases were accomplished with the TRW program.[6] Identical nozzles and inputs were used; the initial value lines were located at the same wall and axis locations, although the locations of intermediate data points differed slightly because of the different line shapes.

It is seen that appreciable differences are obtained from the two calculation techniques, especially in near-wall regions. The main difference in the two flow models is that in the present model all dissipation occurs in the two-phase region of the flow, whereas in the calculation technique of Kliegel-Nickerson[6] the effects of dissipation implicitly are spread throughout the flow. Although performance calculations were not an objective of this investigation, it is interesting to note that the predicted specific impulse is about 1.5% higher in the present calculation (and 0.8% higher for 1-μ particles; 2.2% higher for 3-μ particles).

Typical computing time for a five-iteration solution of an 11×16 array is 1 min on the CDC 6500 computer. The first iteration typically gives gas phase properties within $\frac{1}{2}\%$ of their final values and particle phase properties within 1% of the third-iteration values. Little improvement is found beyond the third iteration. After a sufficient number of iterations, depending upon the degree of departure of the two-phase flowfield from the EGPM initial conditions, some property values become locally erratic. Fluctuating property values appear first at the nozzle exit, particularly in the vicinity of the limiting particle streamline. This behavior indicates that the numerical method of solution and the computer program itself have limitations associated with numerical accuracy and stability. The degree of nonequilibrium in the flowfield is the primary factor controlling the behavior of the solutions and the capability to obtain satisfactory convergence. At the present time, the case of 3-μ particles flowing in a radius ratio one nozzle of the nominal size considered here represents the amount of nonequilibrium that can be handled comfortably. A number of suggestions given in Ref. 8 should improve this limitation if necessary.

Conclusions

1) The gas-particle flow model and analytical method developed here provide an improved analysis of transonic two-phase nozzle flows. The coupled two-dimensional effects of particle size, nozzle radius ratio, details of the nozzle contour, and other parameters on the local behavior of gas-particle flowfields can be determined with this method.

2) The distribution of thermodynamic properties for the gas and particle phases throughout a two-phase flowfield depends primarily on particle size, secondarily on nozzle radius ratio and, to a lesser extent, on the details of the throat contour.

3) Calculations with the present method indicate that the assumption that the local gas phase properties are independent of two-dimensional particle behavior does not adequately represent the gas properties near the nozzle wall where two-dimensional effects are most significant.

4) The calculated downstream properties of a two-phase flow through a nozzle are sensitive to initial value line data. The major difference between the present calculations and previously developed techniques occurs because the effects of dissipation are concentrated in the two-phase region of the flow rather than distributed throughout the flowfield.

References

[1] Hopkins, D. F. and Hill, D. E., "Effect of Small Radius of Curvature on Transonic Flow in Axisymmetric Nozzles," *AIAA Journal*, Vol. 4, No. 8, Aug. 1966, pp. 1337–1343.

[2] Back, L. H., Massier, P. F., and Gier H. L., "Comparison of Measured and Predicted Flows through Conical Supersonic Nozzles, with Emphasis on the Transonic Region," *AIAA Journal*, Vol. 3, No. 9, Sept. 1965, pp. 1606–1614.

[3] Zupnik, T. F., ed., *User's Manual for Subsonic-Transonic Flow Analysis, PWA-2888, Deck 4*, June 1967, Pratt and Whitney Aircraft Div., United Aircraft Corp., East Hartford, Conn.

[4] Friedrichs, K. O., "Theoretical Studies on the Flow Through Nozzles and Related Problems," AMG-NYU Rept. 43, April 1944, New York Univ.

[5] Saunders, L. M., "Numerical Solution of the Flow Field in the Throat Region of a Nozzle," Propulsion Dept. Rept. R-66-3, Aug. 1966, Propulsion and Vehicle Engineering Lab., George C. Marshall Space Flight Center, Huntsville, Ala.

[6] Kliegel, J. R. and Nickerson, G. R., "Axisymmetric Two-Phase Perfect Gas Performance Program," Rept. 02874-6006-R000, Vols. I and II, April 1967, TRW Systems Group, Redondo Beach, Calif.

[7] Hoffman, J. D., "An Analysis of the Effects of Gas-Particle Mixtures on the Performance of Rocket Nozzles," TM-63-1, JPC 348, Jan. 1963, Jet Propulsion Center, Purdue Univ.

[8] Regan, J. F., Thompson, H. D., and Hoglund, R. F., "Two-Dimensional Analysis of Transonic Gas-Particle Flow Fields in Axisymmetric Nozzles," TM 68-9, JPC 451, Aug. 1968, Jet Propulsion Center, Purdue Univ.

[9] Kliegel, J. R. and Nickerson, G. R., "Flow of Gas-Particle Mixtures in Axially Symmetric Nozzles," *ARS Progress in Astronauitcs and Rocketry: Detonation and Two-Phase Flow*, Vol. 6, edited by S. S. Penner and F. A. Williams, Academic Press, New York, 1962, pp. 173–194.

[10] Fox, L., *Numerical Solution of Ordinary and Partial Differential Equations*, Pergamon Press, London, 1962.

[11] Kliegel, J., "Gas Particle Nozzle Flows," *Ninth Symposium (International) on Combustion*, Academic Press, New York, 1963, pp. 811–826.